This full text paper was peer reviewed at the direction of IEEE Communications Society subject matter experts for publication in the WCNC 2009 proceedings.

A Closed Concept for Synchronization and Cell Search in 3GPP LTE Systems

Konstantinos Manolakis[1], David Manuel Gutiérrez Estévez[1], Volker Jungnickel[1]
Wen Xu[2], Christian Drewes[2]
[1] Fraunhofer Institute for Telecommunications, Heinrich-Hertz-Institut
Einsteinufer 37, 10587 Berlin, Germany
[2] Infineon Technologies AG, Am Campeon 1-12, 85579 Neubiberg, Germany
Email: Konstantinos.Manolakis@hhi.fraunhofer.de

***Abstract*—In this paper we investigate the time and frequency synchronization as well as the sector and cell search for the 3GPP Long Term Evolution (LTE) downlink. The proposed algorithms rely on the synchronization and cell-specific reference signals and are hence compliant to most recent 3GPP specifications. Time and (fractional) frequency offset coarse synchronization are performed in the time domain with the cyclic prefix based autocorrelation, while the sector and cell as well as the integer frequency offset are estimated in the frequency domain by using the primary and secondary synchronization signals. To improve the cell detection reliability, the estimated cell is afterwards confirmed through the cell-specific reference signal. All algorithms are evaluated under multipath channel conditions and an initial carrier frequency mismatch. Compromising high performance with reasonable implementation complexity, we draw a practical solution for an LTE receiver.**

***Index Terms*—3GPP LTE, synchronization, cell search, OFDM**

I. Introduction

The Long Term Evolution (LTE) is a new oder mobile communication standard being specified by the 3GPP within Release 8 [1]. This air interface is based on OFDMA in downlink and SC-FDMA in uplink. It offers favorable features such as high spectral efficiency, robust performance in frequency selective channel conditions, simple receiver architecture, etc.

However, it is well known that OFDM systems are sensitive to time and frequency synchronization errors, hence require accurate synchronization for interference-free data reception. Furthermore, when a user equipment (UE) operates in a cellular system, it needs to establish connection as fast as possible with the best serving base station, i.e. to identify the operating sector and cell.

Time and frequency synchronization for 3GPP LTE has been investigated in [2], where a method for generating repetitive synchronization signals and a detection algorithm are described. Cell search based on these proposed synchronization signals is considered in [3]. In [4], dedicated sequences for synchronization and cell search are proposed and evaluated for an LTE system.

In the meantime, synchronization and reference sequences were specified by the 3GPP (see [5]) and the studies mentioned above are not LTE compliant any more. Some of the authors of this paper have published a study on synchronization and sector identification [6] under consideration of the recent specifications, as in [5]. In the current paper we improve sector search and furthermore study the cell search and cell identification resulting finally in a closed concept for a 3GPP compliant receiver.

In the following Section, the 3GPP LTE synchronization and cell-specific reference signals are briefly described, while Section III presents the system model. In Section IV, time and frequency synchronization are considered and in Section V sector and cell search are discussed. The cell confirmation and the complete procedure are presented in Section VI while the individual blocks and overall performance are evaluated in Section VII, before conclusions are drawn in Section VIII.

II. LTE Synchronization and Reference Signals

According to 3GPP LTE specification [5], downlink transmission is organized into radio frames with a duration of $10ms$. Each radio frame consists of 10 sub-frames, each with two consecutive $0.5ms$ slots. Data are mapped on a time-frequency resource grid consisting of elementary units called resource elements. They are uniquely identified by the transmit antenna, the sub-carrier position and the OFDM symbol index within a radio frame.

A. Synchronization signals

A dedicated synchronization channel (SCH) is specified in LTE [5] for transmitting two synchronization signals, the primary (P-SCH) and the secondary (S-SCH). Within the SCH, both synchronization sequences are mapped on 62 sub-carriers located symmetrically around the DC-carrier. They are transmitted within the last two OFDM symbols of the first and sixth sub-frame (sub-frame index 0 and 5), i.e. every $5ms$.

The P-SCH signal consists of three length-62 Zadoff-Chu sequences in frequency domain which are orthogonal to each other. Each sequence corresponds to a sector identity $N_s = 0,1$ or 2 within a group of three sectors (physical cell).

The S-SCH signal consists of a frequency-domain sequence $d(n)$ with the same length as the P-SCH, which is an interleaved concatenation of the two length-31 binary sequences $s_0(n)$ and $s_1(n)$. In order to distinguish between different sector groups (physical cells), $s_0(n)$ and $s_1(n)$ depend on a pair of integers m_0 and m_1, which are unique for each

978-1-4244-2948-6/09/$25.00 ©2009 IEEE

Authorized licensed use limited to: Yonsei University. Downloaded on May 30, 2009 at 01:06 from IEEE Xplore. Restrictions apply.

group-ID N_g (from 0 to 167). The concatenated sequences are scrambled with one of the sequences $c_0(n)$ and $c_1(n)$, which are cyclic shifted versions of the length-31 binary sequence $\tilde{c}(n)$. The shift value is depending on the sector-ID N_s, while a constant shift of 3 samples holds between $c_0(n)$ and $c_1(n)$. Further, a pair of scrambling sequences $z_1^{m_0}(n)$ and $z_1^{m_1}(n)$ (cyclic shifted versions of sequence $\tilde{z}(n)$), which also depend on N_g is multiplied with the odd entries of the S-SCH. In order to enable the detection of beginning of radio frame, the S-SCH signal is different for each sub-frame index (0 or 5), thus the final S-SCH sequence $d(n)$ is given by

$$d(2n) = \begin{cases} s_0^{m_0}(n)c_0(n) & \text{in sub-frame 0} \\ s_1^{m_1}(n)c_0(n) & \text{in sub-frame 5} \end{cases}$$

$$d(2n+1) = \begin{cases} s_1^{m_1}(n)c_1(n)z_1^{m_0}(n) & \text{in sub-frame 0} \\ s_0^{m_0}(n)c_1(n)z_1^{m_1}(n) & \text{in sub-frame 5} \end{cases}$$

As $d(n)$ is real valued, time domain symmetry always holds for the S-SCH signal.

The overall cell-ID N_c (from 0 to 503) is equal to

$$N_c = 3N_g + N_s \ , \tag{1}$$

is thus defined by the sector and group identities N_s and N_g.

B. Cell-specific reference signals

Cell-specific reference sequences $P(n)$ (defined in [5]) consist of complex-valued entries defined by

$$P_{l,n_s}(n) = \frac{1}{\sqrt{2}}(1-2\cdot c(2n)) + j\frac{1}{\sqrt{2}}(1-2\cdot c(2n+1)) \tag{2}$$

for $n = 0, ..., 2N_{RB}^{max} - 1$, where N_{RB}^{max} is the maximum number of resource blocks, n_s is the slot index within the radio frame and l is the OFDM symbol index within the slot. The pseudo random sequence $c(n)$ is generated by a length-31 Gold sequence, the state of which is initialized by c_{init} at the beginning of each OFDM symbol. The initializing value is given by

$$c_{init} = 2^{10}\cdot(7\cdot(n_s+1)+l+1)\cdot(2\cdot N_c+1)+2\cdot N_c+N_{CP} \tag{3}$$

where

$$N_{CP} = \begin{cases} 1 & \text{for normal cp} \\ 0 & \text{for extended cp} \end{cases}$$

Equation 3 indicates that $c(n)$ and consequently the reference sequence $P(n)$ are unique for each slot, OFDM symbol and cell index, and as well depend on the cyclic prefix type (short/long).

The sequence elements are mapped on the time-frequency resource grid on every sixth sub-carrier within two OFDM symbols in every slot. In case of multiple transmit antennas, resource elements used for the reference signal transmission shall not be used for transmission on any other antenna in the same slot and are thus set to zero. An example for the allocation of the reference sequences within the resource grid is illustrated in Figure 1.

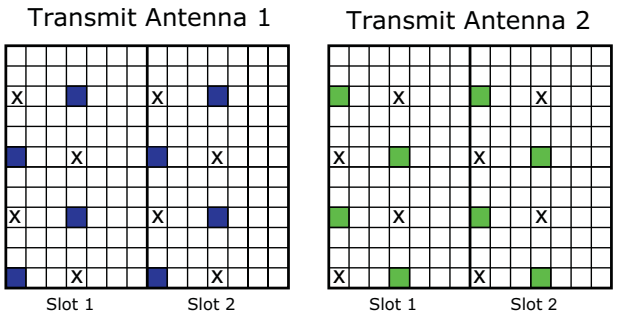

Fig. 1. Cell-specific reference signals for two transmit antennas. Sequences are mapped on colored resource elements, X-sub-carriers are set to zero. The grid shall be shifted in frequency direction according to the cell-ID (horizontally: time, vertically: frequency).

III. System Model

We consider the transmission of a serial discrete baseband OFDM stream $s(n)$ given by

$$s(n) = \frac{1}{\sqrt{N}}\sum_{k=0}^{N-1} X_k e^{j2\pi kn/N} \ , 1 \le n \le N \tag{4}$$

where X_k denotes the modulated data on the k^{th} sub-carrier and N the FFT size. Transmitting over a multipath propagation channel under consideration of a frequency misalignment between transmitter and receiver oscillators as well as additive white Gaussian noise (AWGN), the received signal will be

$$r(n) = [s(n) \otimes h(n) + w(n)]e^{j2\pi\varepsilon n/N} \ , \tag{5}$$

where $h(n)$ is the channel impulse response (CIR), ε denotes the frequency mismatch with respect to the sub-carrier spacing, $w(n)$ is the noise term and $\otimes$ stands for the linear convolution. The CIR is modeled as

$$h(n) = \sum_{d=0}^{N_d-1} h_d\delta(n-d) \tag{6}$$

where N_d is the number of channel taps and h_d the complex value of the d-th Rayleigh-distributed tap. The mean power of h_d follows an exponential decay and is given by

$$\sigma_d^2 \sim e^{-\frac{d}{\tau}} \ , \tag{7}$$

where τ is the power decay constant.

After applying the N-point FFT at the receiver and assuming perfect timing, the OFDM symbol is given by

$$Y_l = \frac{1}{\sqrt{N}}\sum_{n=0}^{N-1} r(n)e^{-j2\pi ln/N} =$$

$$= \frac{1}{N}\sum_{k=0}^{N-1} H_k X_k \sum_{n=0}^{N-1} e^{2\pi n(k-l+\varepsilon)/N} + W_k \tag{8}$$

with

$$H_k = \sum_{l=0}^{N_l-1} h_l e^{-j2\pi kl/N} \text{ and } W_k = \frac{1}{\sqrt{N}}\sum_{n=0}^{N-1} w(n)e^{-j2\pi nk/N} \ . \tag{9}$$

Authorized licensed use limited to: Yonsei University. Downloaded on May 30, 2009 at 01:06 from IEEE Xplore. Restrictions apply.

As it can be observed from Equation 8, the received OFDM symbol will be affected not only by the channel and noise distortions H_k and W_k, but also by a term due to the CFO (ε). According to [7], the within the received OFDM symbol Y_l constellation will be rotated by an equal phase known as the common phase error (CPE), which is independent of the particular sub-carrier. Furthermore, the loss of orthogonality between sub-carriers has a noise-like effect called inter-carrier interference (ICI) (see [7]).

IV. Time and Frequency Synchronization

The objective of synchronization is to retrieve OFDM symbol timing and to estimate the carrier frequency offset (CFO). The CFO can be separated into an "integer" part, which is a multiple of the sub-carrier spacing, and a "fractional" part, which is responsible for the CPE and ICI. The CFO regarding the sub-carrier spacing can be thus given as

$$\varepsilon = n_I + \varepsilon_F \ , \tag{10}$$

where n_I is the integer number of sub-carrier spacings and ε_F the fractional part with $-1 < \varepsilon_F < 1$. In [6] we investigated several approaches on time and frequency synchronization for LTE. According to conclusions of this study, we decide to use the cyclic prefix based method for acquisition of the OFDM symbol timing and the fractional CFO, as it is originally proposed in [8]. The log-likelihood function for the OFDM symbol start (θ) and the frequency mismatch (ε_F) can be written as

$$\Lambda(\theta, \varepsilon_F) = 2|\gamma(\theta)|cos\{2\pi\varepsilon_F + \angle\gamma(\theta)\} - \rho\mathcal{E}(\theta) \ . \tag{11}$$

In Equation 11, $\angle$ denotes the argument of a complex number,

$$\gamma(n) \equiv \sum_{k=n}^{n+L-1} r(k)r^*(k+N) \tag{12}$$

is the correlation term and

$$\mathcal{E}(n) \equiv \sum_{k=n}^{n+L-1} |r(k)|^2 + |r(k+N)|^2 \tag{13}$$

the energy term, while L denotes the CP length, measured in time samples. The magnitude of the correlation coefficient between $r(k)$ and $r(k+N)$ is given by $\rho \equiv \frac{\sigma_s^2}{\sigma_s^2+\sigma_n^2}$, where σ_s^2 and σ_n^2 denote the signal and noise power respectively. The maximum likelihood (ML) estimate of θ and ε_F maximizes the function $\Lambda(\theta, \varepsilon_F)$, and is given by

$$\widehat{\theta}_{ML} = \arg\max_{\theta}\{2|\gamma(\theta)| - \rho\mathcal{E}(\theta)\} \tag{14}$$

$$\widehat{\varepsilon}_{F,ML} = -\frac{1}{2\pi}\angle\gamma(\widehat{\theta}_{ML}) \ . \tag{15}$$

The computation of $\gamma(n)$ is a low complexity operation as it can be implemented by following recursive formula

$$\gamma(n+1) = \gamma(n) + r(n+L)r^*(n+L+N) - \\ -r(n)r^*(n+N) \ , \tag{16}$$

while $\mathcal{E}(n)$ can be computed in the same way.

The cyclic prefix based method remains unaffected by the presence of high CFO, but estimates only the fractional part ε_F. Furthermore, it indicates only the OFDM symbol timing, but not the beginning of the radio frame (BOF). The performance of this method can be significantly improved by averaging $\Lambda(\theta, \varepsilon_F)$ over several OFDM symbols [8].

V. Sector and Cell Search

A. Sector search

In order to identify the sector with the highest signal level we perform a cross-correlation of the received symbols on the 62 centered sub-carriers with replicas of the three P-SCH signals in the frequency domain according to

$$Q_i(n) = \sum_{k=-31, k\neq 0}^{31} d_i^*(k)R(n+k) \ , \tag{17}$$

where $d_i(n)$ denotes the replica of the i^{th} P-SCH sequence and $R(n)$ the received symbols. The magnitude of the cross-correlator output $|Q_i(n)|$ corresponding to the sector with the highest signal shows a large peak compared to the other correlation terms due to orthogonality between sequences. Thus, the estimated sector-ID is given by

$$\widehat{N}_s = \arg\max_i(|Q_i(n)|) \ . \tag{18}$$

Simultaneously, the sector identification indicates the radio frame start as the P-SCH position within the radio frame is already known, however with an uncertainty between first and sixth sub-frame. This information is retrieved by decoding the S-SCH signal, as explained in following Section V-B.

B. Group and cell search and integer CFO estimation

The cell-ID needs to be estimated correctly, in order to establish connection with the best possible serving base station. At the same time, the cell-ID is required for extracting the reference sequence entries from proper sub-carrier positions, and perform afterwards a channel estimation via interpolation in frequency domain.

The group-ID N_g can be jointly estimated with the integer CFO n_I and the sub-frame index within the radio frame (0 or 5). The basic concept is to exploit the cyclic shifts of the two length-31 binary sequences $s_0(n)$ and $s_1(n)$ according to the pair of integers m_0 and m_1, which identify the group-ID. The quantity of integer CFO n_I can be estimated by the sub-carrier shift of the sequence $d(n)$. The method proposed here consists of following steps (with same notations as [5]):

- Extract the S-SCH signal according to the estimated OFDM symbol timing and apply an N-point FFT
- Separate 62-length sequence $d(n)$ into sequences $d(2n)$ and $d(2n+1)$, consisting of even and odd sub-carrier symbols

In the following we use the notation for sub-frame 0:

Authorized licensed use limited to: Yonsei University. Downloaded on May 30, 2009 at 01:06 from IEEE Xplore. Restrictions apply.

- Divide $d(2n)/c_0(n)$ in order to obtain the sequence $s_0^{(m_0)}(n)$. Sequence $c_0(n)$ is known at the receiver as it depends only on the already estimated sector-ID N_s.[1]
- Build a reference sequence $s_{ref}(n)$, which is a duplicated version of $s_0^{(m_0=0)}(n)$ with the length of 62.
- Apply a cross-correlation between $s_0^{(m_0)}(n)$ and the reference sequence $s_{ref}(n)$. The magnitude of the correlation term shows a significant maximum between sample 32 and 62, which indicates $m_0 = 31 - index_{max}$, as illustrated in Figure 2.
- After estimating the integer m_0, we are able to compute $z_1^{(m_0)}(n)$ and afterwards divide $d(2n+1)/(c_1(n)z_1^{(m_0)}(n))$ in order to obtain the sequence $s_1^{(m_1)}(n)$.
- Apply a cross-correlation between $s_1^{(m_1)}(n)$ and $s_{ref}(n)$. The magnitude of the correlation term shows a significant maximum between the 32-th and 62-th sample, which indicates $m_1 = 31 - index_{max}$, as illustrated in Figure 2.
- The pair of estimated m_0 and m_1 identifies the group-ID N_g.
- Compute the overall cell-ID: $N_c = 3N_g + N_s$.

The described procedure is performed for several cyclic shifts of $d(n)$ (for instance a shift of -2 to $+2$ sub-carriers), in order to detect the integer CFO part n_I. Significant peaks will only be generated if the received sequence $d(n)$ is positioned on the correct frequency grid. Figure 2 shows an example of correlation magnitudes for estimating integers m_0 and m_1. Side peaks located outside the detection interval are not considered as main peaks.

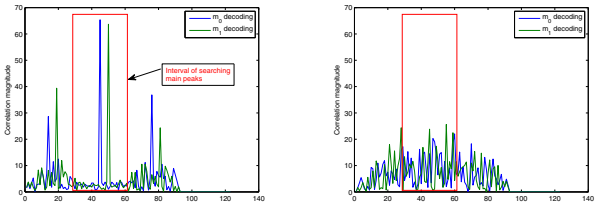

Fig. 2. S-SCH sequence decoding for retrieving group-ID N_g, sub-frame index and integer CFO n_I. *Left*: Significant peaks clearly indicate the case of correct N_g, sub-frame index and n_I. *Right*: Correlation magnitude in case of inappropriate cyclic shift.

In our concept the cell search algorithm has to cope with the distortion through channel, non-perfect timing as well as a possible integer CFO, which is not yet detected. The fractional CFO can usually be estimated by the CP based method and can be compensated by a multiplication of the signal with a conjugate oscillation in the time-domain.

VI. Cell Confirmation

After having estimated the cell through the P-SCH and S-SCH signals, we verify this estimate by the cell-specific reference signals with a cross-correlation based procedure in the frequency domain. As the channel equalization is not feasible yet, the received reference sequences will be affected by the channel frequency response which may corrupt the cross-correlation. In order to overcome this obstacle, we intend to eliminate the channel effect on the received sequences by applying a method as described in [4]. If the spacing between two reference symbols is smaller than the channel coherence bandwidth, the channel responses on these sub-carriers can be considered as correlated. By applying a differential modulation on the received reference sequences, we practically eliminate the channel phase effect, which mainly degrades the correlation performance (reference sequence elements have a magnitude of 1). Afterwards, we perform the same operation to the actual sequences which correspond to the estimated cell and apply a cross-correlation according to

$$C(n) = \frac{\sum_{l=1}^{N_{sym}} \sum_{k=1}^{N_{ref}-1} Y(n+k+1,l)Y^*(n+k,l)P^*(k+1,l)P(k,l)}{\sum_{l=1}^{N_{sym}} \sum_{k=1}^{N_{ref}-1} |Y(k,l)|^2}. \quad (19)$$

In Equation 19 $P(k,l)$ and $Y(k,l)$ denote the k^{th} entry of transmitted and received reference sequences in the l^{th} OFDM symbol of a slot. N_{ref} is the length of the reference sequences (depends on the transmission bandwidth) and $N_{sym} = 2$ is the number of OFDM symbols containing reference sequences within a slot (see [5]).

The magnitude $|C(n)|$ is expected to show a centrally located high peak when the cell-ID was correctly estimated. In the opposite case, a correlation will be performed between two unequal reference sequences or between a reference sequence and received data. Thus, $|C(n)|$ will not show a significant peak and the estimated cell-ID shall be considered as false. Both cases are illustrated in Figure 3 for the AWGN case.

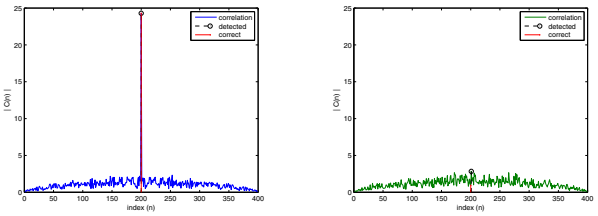

Fig. 3. Cell-ID confirmation through cross-correlation with reference sequences. Magnitude peak indicates whether cell-ID was correctly estimated (left) or not (right). Results for the AWGN channel, SNR=10 dB.

Finally, we construct a procedure including time and frequency synchronization, sector and cell search, and cell identification, as illustrated in Figure 4. Blocks are adjusted to each other and feedback control signals guarantee the stability of this receiver sub-system. If the S-SCH signal decoder fails several times, the synchronization will be refreshed, as a wrong sector-ID or large synchronization errors occur. Similarly when the estimated cell is not confirmed after several iterations, which means that sector or group were estimated

[1] An incorrect sector estimation automatically causes an error in group estimation, due to inappropriate $c_0(n)$ and $c_1(n)$ sequences.

Authorized licensed use limited to: Yonsei University. Downloaded on May 30, 2009 at 01:06 from IEEE Xplore. Restrictions apply.

falsely, the complete process is performed from the beginning.

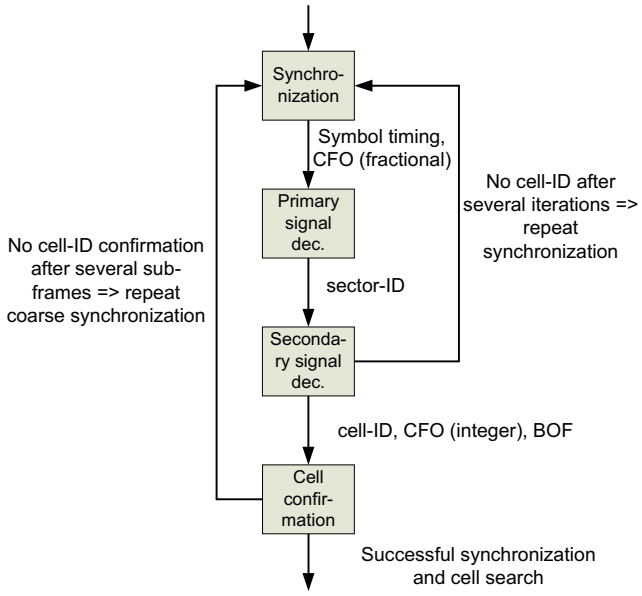

Fig. 4. The procedure including time/frequency synchronization, sector/cell search and identification. Adjustments between blocks and feedback control signals guarantee stable operation.

VII. Performance Evaluation

We carried out link level simulations for evaluating the performance of the presented algorithms. The $20MHz$ LTE system (see [9]) was considered, with a sampling frequency of $30.72MHz$, 2048-point FFT/IFFT, 144-sample ($\approx 4.9\mu s$) CP and a $15kHz$ sub-carrier spacing. We considered one antenna at transmitter and receiver. The maximum channel delay spread was $1.3\mu s$, which corresponds to an impulse response of $N_l = 40$ taps by considering the system sampling frequency. Simulations were performed over a sufficient number of sub-frame based transmissions over independent channel realizations for SNR $= -5$ to 15 dB. We also considered a frequency misalignment of $750Hz$, which corresponds to $\varepsilon = 0.05$.

In Figure 5 the root mean square error (RMSE) of the OFDM symbol timing estimation measured in samples is plotted against the SNR. As for the low SNR case the estimate is not accurate, it should be further improved by averaging the function $\Lambda(\theta, \varepsilon_F)$ (see Section IV). Further it can be observed from Figure 5 that for high SNR the curve runs into a floor of a few samples, stemming from the fact that correlation based procedures are triggered by the mean delay of the channel. In fact, such an uncertainty exists in the time synchronization even in a noise-free case.

In Figure 6 the RMSE of frequency estimation for the CP based method is illustrated against the SNR. Coarse estimate shall be further refined by employing tracking algorithms based on the cell-specific reference signals, according to principles as in [7]. As shown in [6], after fine synchronization the residual frequency offset can be reduced to a few Hz.

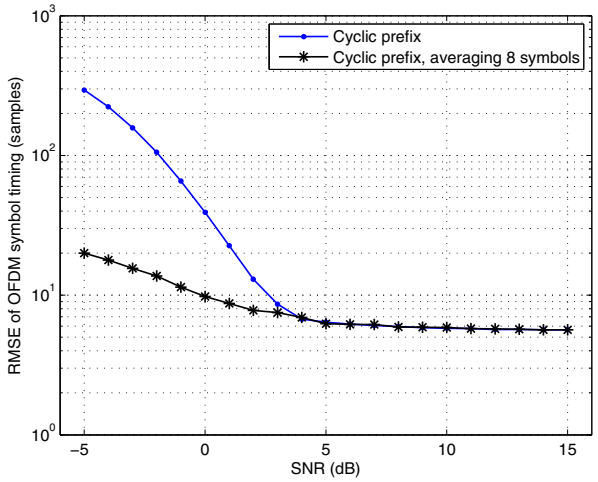

Fig. 5. Coarse time synchronization in terms of the RMSE vs. the SNR, measured in samples. Estimation accuracy is limited by the channel delay spread.

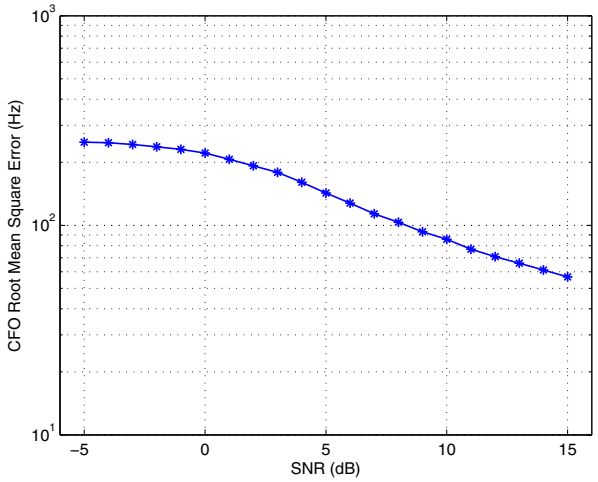

Fig. 6. Coarse frequency synchronization in terms of the RMSE vs. the SNR, measured in Hz.

After having retrieved the OFDM symbol timing, the cyclic prefix is removed accordingly and the N-point FFT is applied. For the P-SCH cross-correlation (see Section V-A), when using an energy depending threshold to exclude incorrect low correlation peaks, there is a certain miss rate. The higher the threshold, the higher the probability that the correct peak does not reach this threshold level. This miss rate is almost equal to the sector fail rate, when an isolated sector/cell environment is considered, as the possibility that one of the other correlation terms generates a peak higher than the peak corresponding to the actual sector is very small. For the sector fail rate we employed an empirical threshold equal to 0.023 of the 62-length received P-SCH sequence energy.

The fail rate in cell estimation is depending on the sector and the group fail rate (Section V-A and V-B respectively).

Authorized licensed use limited to: Yonsei University. Downloaded on May 30, 2009 at 01:06 from IEEE Xplore. Restrictions apply.

When the sector is false, the group is automatically estimated wrongly, according to the S-SCH signal decoding algorithm in Section V-B. Further, it might be possible that the group-ID is estimated wrongly, even when the sector-ID was correctly estimated. Hence, the fail rate of the overall cell-ID should be at least as high as the sector miss rate. Figure 7 illustrates all three rates, where the group fail rate appears to be very small. This means that the S-SCH decoding process is successful, even under conditions of multipath channel and realistic time and frequency synchronization. If sector information is correctly acquired by the P-SCH signal, the cell is estimated correctly in most cases.

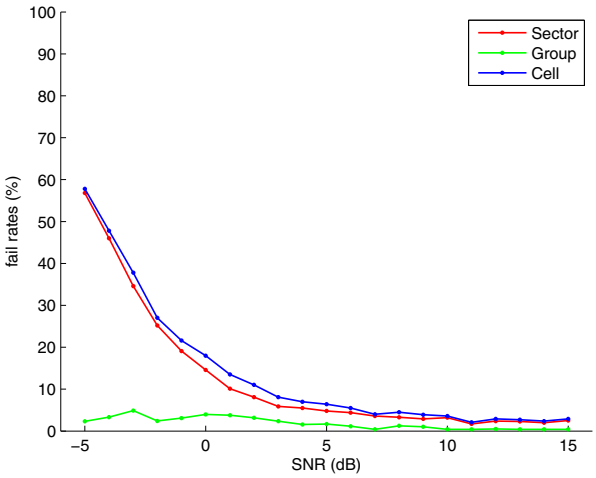

Fig. 7. Fail rate (%) of P-SCH signal when threshold equal to to 0.023 of the received P-SCH sequence energy, fail rate of S-SCH signal decoding (group miss rate) and resulting cell fail rate. When sector information is correctly acquired, the cell is estimated correctly in most cases.

The performance of the cell identification process is evaluated in Figure 8 in terms of the fail rate (%), i.e. the percentage of not sucessful cell confirmations when the cell was correctly estimated by the S-SCH signal. It can be observed that as a consequence of channel distortion, the fail rate curve runs into a floor of about 4% when not using differential modulation before cross-correlation, even by assuming perfect synchronization. When performing the cross-correlation combined with differential modulation according to Equation 19, the miss rate almost reaches zero, even under realistic synchronization conditions. We can thus conclude that the described approach provides a reliable check of the cell estimate.

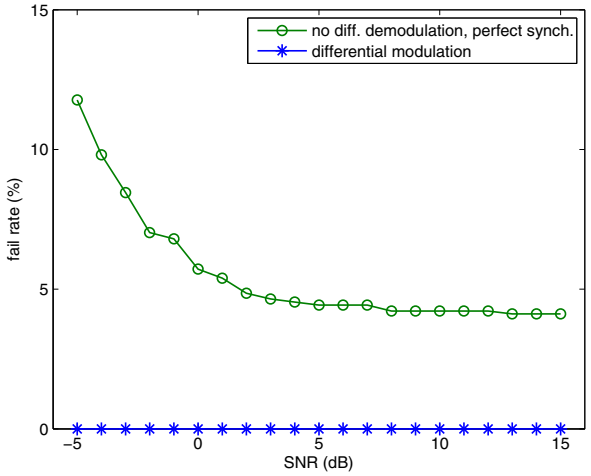

Fig. 8. Fail rate of the cell confirmation process in case of initial correct cell estimation. Cross-correlation a) without differential modulation and by assuming perfect synchronization and b) with differential modulation under realistic synchronization conditions.

VIII. Conclusion

For a 3GPP LTE receiver, cross-correlation needs to be performed to estimate the sector-ID and enable cell identification. It also provides a reliable estimate of the beginning of frame. However, for timing acquisition the low-complexity cyclic prefix based autocorrelation should be preferred, as it is not influenced by frequency errors. In this work, estimation of large frequency offset and cell search are jointly performed with the secondary synchronization signal, while the cell-ID estimates are confirmed through the cell-specific reference signals. The complete procedure enables a robust connection to the base station at a reasonable implementation complexity.

References

[1] 3GPP TS 36.300 V8.5.0: "Evolved Universal Terrestrial Radio Access (E-UTRA) and Evolved Universal Terrestrial Radio Access Network (E-UTRAN); Overall description", May 2008.

[2] Yinigmin Tsai and Guodong Zhang, "Time and Frequency Synchronization for 3GPP LTE Long Term Evolution Systems", *IEEE Vehicular Technology Conference, 65th VTC2007-Spring*, April 2007.

[3] Yinigmin Tsai, Guodong Zhang, Donald Grieco, Fatih Ozluturk, "Cell Search in 3GPP Long Term Evolution Systems", *IEEE Vehicular Technology Magazine*, vol. 2, issue 2, June 2007.

[4] SU Huan, Zhang Jian-hua, "Cell search algorithms for the 3G long-term evolution", *The Journal of China Universities of Posts and Telecommunications*, vol. 14, issue 2, June 2007.

[5] 3GPP TS 36.211 V8.4.0: "Physical channels and modulation", September 2008.

[6] K. Manolakis and V. Jungnickel, "Synchronization and Cell Search for 3GPP LTE", *13th International OFDM Workshop (InOWo'08)*, August 2008.

[7] M. Speth, S.A. Fechtel, G. Fock and H. Meyr, "Optimum Receiver Design for Wireless Broad-Band Systems Using OFDM - Part I", *IEEE Trans. Communications*, vol.47, no. 11, November 1999.

[8] M.Sandell, J.J. v.d. Beek and P.O.Börjesson, "Timing and Frequency Synchronization in OFDM Systems Using the Cyclic Prefix", *Proc. IEEE Int. Symp. Synchronization*, Essen, Germany, Dec. 1995.

[9] 3GPP TR 25.814 V7.1.0: "Physical layer aspects for evolved Universal Terrestrial Radio Access (UTRA)", September 2006.

Authorized licensed use limited to: Yonsei University. Downloaded on May 30, 2009 at 01:06 from IEEE Xplore. Restrictions apply.